Impact of the MRI-based Navigation System Constraints on the Step Response Using a PID Controller

Samer Tamaz[1], Sylvain Martel[1*]
[1]NanoRobotics Laboratory, Department of Computer Engineering and Institute of Biomedical Engineering,
École Polytechnique de Montréal (EPM), Campus of the Université de Montréal, Montréal (Québec) Canada

*E-mail: sylvain.martel@polymtl.ca URL: www.nano.polymtl.ca

***Abstract*—This paper presents the identification and the study of the impact of a real-time MRI-based propulsion and tracking system constraints on the step response using a discrete PID controller. A simplified model for such a system accounts for these constraints which are the time delay, the sampling period, and the blood velocity. This application is intended for minimally invasive operations within the human cardiovascular system.**

Keywords—**Feedback motion control, real-time, MRI, time delay, fluid drag, magnetic propulsion, microdevice**

I. Introduction

The MR-Sub (Magnetic Resonance Submarine) project consists in guiding and propelling a microdevice in the human cardiovascular system using a clinical Magnetic Resonance Imaging (MRI) platform for medical purposes [1,2]. Catheters being limited by their radius of curvature are unable to reach remote areas within the cardiovascular system. The MR-Sub offers a technique that could compensate for such a constraint. The cleverness of this approach consists in extracting the propelling and tracking means from the microdevice to alleviate it and make it as small as possible in order to reach blood vessels as small as capillaries [3,4]. Furthermore, this eliminates the risk of malfunction of the embedded propelling and tracking units. Instead, the microdevice will be equipped with a ferromagnetic core, susceptible of being localized by MRI, on which magnetic gradients generated by the MRI coils will act to propel it. The feedback control strategy for such a system is quite challenging since it will have to ensure that the microdevice evolves in a physically constrained environment where size and sinuosity must be accounted for. More specifically, the microdevice will have to move into blood vessels whose diameters vary approximately from few µm in capillaries to 3 cm in the aorta. To deal with the winding of the vessels, a pre-acquired roadmap will identify and segment the path to allow a feedback control over segments as linear as possible [5]. In summary, along each fragment of the path segmented by the roadmap, and based on the distance which separates the targeted position from the current position of the microdevice, the compensator will have to determine the appropriate amplitude of the magnetic gradients along each direction, in order to bring the microdevice to destination.

II. Methodology

Due to complexity of the anatomical environment in which the microdevice will have to progress, a step-by-step approach is adopted in order to reach the optimal design of the system. First, a simplified model is considered. Second, the results obtained by the simulation of the open-loop system are compared with the experimental results. If results correlate, a controller is integrated in the closed-loop system and calibrated in order to reach the required criterions. Otherwise, the model transfer function is deduced from experimental results using system identification techniques. This algorithm is then repeated again by adding the next most significant constraint to the model, until the control of a system close to reality is ensured.

II. Modelling

A first proposed simplified model accounts for the horizontal and vertical navigation of a spherical bead in a fluid that would be tested *in vitro*. The bead which is composed of ferromagnetic and non ferromagnetic compounds is subjected to four forces. The magnetic force is defined as:

$$F_m = V_m \cdot (M \cdot \nabla) B \tag{1}$$

where V_m is the magnetic volume, M is the magnetization ferromagnetic compound, and ∇B is the magnetic gradient amplitude. The drag force is expressed as:

$$D = \frac{1}{2} \rho_f \cdot u^2 \cdot A_t \cdot C_D \tag{2}$$

where ρ_f is the fluid density, u is the relative speed between the bead and the fluid, A_t is the cross-section area of the bead, and C_D is the drag coefficient for a sphere defined as:

$$C_{D_\infty} \approx \frac{24}{\mathrm{Re}} + \frac{6}{1+\sqrt{\mathrm{Re}}} + 0.4 \qquad 0 \le \mathrm{Re} \le 2 \times 10^5 \tag{3}$$

Preprint submitted to 27th IEEE EMBS Annual International Conference.
Received May 2, 2005.

In Eq. 3, *Re* is the Reynolds number defined as:

$$\mathrm{Re} = \frac{\rho_f . u . d_t}{\mu} \tag{4}$$

where μ is the fluid viscosity, and d_t the diameter of the bead. The infinite sign in Eq. 3 denotes that the expression ignores the presence of an enclosed environment in which the bead will progress. A constant fluid speed was considered. The buoyancy force:

$$\mathrm{b} = \mathrm{V_t} \cdot \rho_f \cdot \mathrm{g} \tag{5}$$

where V_t is the total volume of the bead, and g is the gravitational constant. The weight of the bead is defined as:

$$\mathrm{W} = \mathrm{V_t} \cdot (\rho_m + \rho_n) \cdot \mathrm{g} \tag{6}$$

where ρ_m is the mass density of the ferromagnetic compound, and ρ_n is the mass density of the non ferromagnetic compound of the bead.

The buoyancy force and the weight apply only to the vertical motion. Without loss of generality, friction forces generated between the bead and the enclosed environment bores are ignored here since a state of buoyancy is assumed. This state is ensured by the combination of the buoyancy force along with the upward magnetic force. The ferromagnetic compound used is the Permendur for its high saturation magnetization of 1.9496 x 10^{-6} A/m whose density is 8.12 g/cm^3. A non ferromagnetic compound of equal density and null magnetization is chosen to reflect the worst case scenario of the future microdevice. The opted volume of the bead is 13.6 cm^3, to be conformed to the characteristics of the bead that was used for the latest localization experiments. As for the fluid, the blood characteristics where chosen to reflect the cardiovascular environment. Its density is 1.05 g/cm^3 approximately and viscosity is 0.0035 P.

Besides these forces, six meaningful constraints related to the 1.5 T Siemens Avanto clinical MRI system (used for the experimental tests) have to be taken into account. First and foremost, the maximum peak-to-peak magnetic gradient is 80 to 90 mT/m along the horizontal axis, and 80 mT/m along the vertical axis. For simulation purposes, a maximum peak-to-peak magnetic gradient of 174 mT/m was assumed for the vertical axis, a value just enough to pull the bead upward in a null flow. Second, in order to avoid overheating of MRI gradient coils, a duty cycle of 10 ms ON / 2 ms OFF is considered. This is equivalent to 83 % of the available magnetic force with a 100 % duty cycle. Third, the estimated minimal time required by a novel positioning technique (developed in our laboratory) to apply a special pulse sequence (t_{gpos}) in order to acquire the unidirectional dynamic position of the bead is 8 ms. Fourth, until now, it has not been proven that the gradients for positioning can be generated simultaneously with the magnetic propulsion gradients, therefore, the generation of the first gradients must be cancelled during the generation of the latter ones, and *vice versa*. This constraint is designated by the dead-time (*DT*). Fifth, the delay (*d*) is the sum of the required time to determine the coordinates of the position (t_{coord}), to perform the task of the controller (t_{cont}), and to convey the information between the different units of the system (t_{com}). These equates to an estimated delay of 12 ms where t_{com} predominates. Sixth, a maneuvering area of 40 cm in radius which delimits the homogeneity region of the MRI system must be respected.

II. Controller

Initially, a PID controller with filtered derivative is selected for its simplicity and the ease to identify the impact of the forces and constraints on the system response. Its transfer function is expressed in Laplace transform as:

$$\mathrm{K(s)} = \frac{\mathrm{U(s)}}{\mathrm{E(s)}} = K_p \left(1 + \frac{1}{T_i s} + \frac{T_d s}{1 + \frac{T_d}{N} s} \right) \tag{7}$$

where U represents the command, E is the distance separating the targeted position of the bead from its current position, K_P is the proportional gain, T_i is the integration time, T_d is the derivative time, N is the fraction of command signal high frequency limiter of derivative action [6]. The digital transfer function of (5) is expressed by:

$$\mathrm{K(z)} = K_p \left(1 + \frac{\frac{h}{K_i}}{z-1} + \frac{N(z-1)}{\left(1 + N\frac{h}{K_d}\right) z - 1} \right) \tag{8}$$

where the following z-transform is applied along with Euler's approximation methods [7]:

$$\mathrm{K(z)} = (1 - z^{-1}) Z\left[L^{-1}\left[K(s)/s \right] \right] \tag{9}$$

To reduce the windup effect generated by the integral gain, a saturation block corresponding to the anti-windup was included. In (6), h denotes the sampling period for a proper feedback control that abide by:

$$h \geq t_{gpos} + d \tag{10}$$

Preprint submitted to 27th IEEE EMBS Annual International Conference.
Received May 2, 2005.

A trial and error method [8] was used to tune the PID parameters based on transient step response specifications, and led to the following settings: $K_P = 6.5$, $T_i = 5$, $T_d = 0.04$, and $N = 10$. A target of 10 cm away from the starting point is chosen with the available physical constraints mentioned in the preceding section. This distance represents the fragment's distance determined by the roadmap. Although the importance of transient response specifications is not apparent for unidirectional path, these must be taken into account since they will be significant when dealing with 2D and 3D paths. Among the several specifications identified by [9], the steady state error (e_{ss}), the maximum percent overshoot (M_P), the ripples (*rip*) peak-to-peak amplitude, and a reasonable rise time (t_r) where taken into consideration (enumerated by order of importance).

III. Results

When propelled from rest along the horizontal axis with a maximum magnetic gradient of 40 mT/m, the bead can sustain an opposite fluid speed of 39.8 cm/s approximately where only the duty cycle is being considered among the cited constraints. This speed value was determined through open-loop simulations using Matlab/Simulink. The results presented here were generated using a variable-step continuous solver along with an ode45 integration method. An automatic maximum step size was chosen since the processing time of the computer architecture discussed in [10] is currently unknown. Ripples of less than 1 μm in amplitude were ignored. In the presence of ripples, an average e_{ss} was computed. The Simulink block diagram of the discrete closed-loop control system is illustrated in Fig. 1.

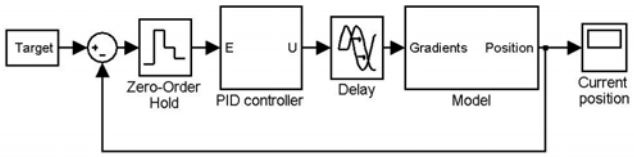

Fig. 1. Block diagram of the discrete closed loop control system.

IV. Discussion

Fig. 4 depicts the impact of the fluid speed on the step response. A negative speed indicates that the bead is moving opposite to the direction of the flow to reach the target, whereas a positive speed indicates that the bead's direction is the same as the flow direction. That explains the absence of overshoot for negative speed, where the controller immediate reaction is tempered by the opposing flow direction. Fig. 2, shows that as the delay gets closer to the sampling frequency, the step response is drastically deteriorated. By comparing Fig. 2 to Fig. 3, it can be inferred that, as the delay is increased, the *DT* accelerates the emergence of the response deterioration. Fig. 5 emphasizes the importance of the sampling period which is the parameter that must be determined by the control designer to reach an optimal navigation. The results for the vertical positioning were not included here since they correlate with those of horizontal positioning. This correlation is foreseen since the additional forces considered vertically are linear.

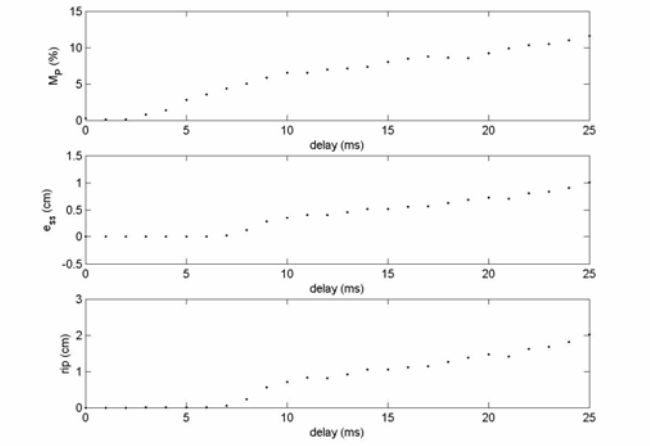

Fig. 2. Maximum percent overshoot (M_P), steady state error (e_{ss}), ripples *(rip)* peak-to-peak amplitude as a function of the delay of the step response, where d = 0, with duty cycle, without DT, $v_f = 0$, h = 25 ms, for a horizontal propulsion.

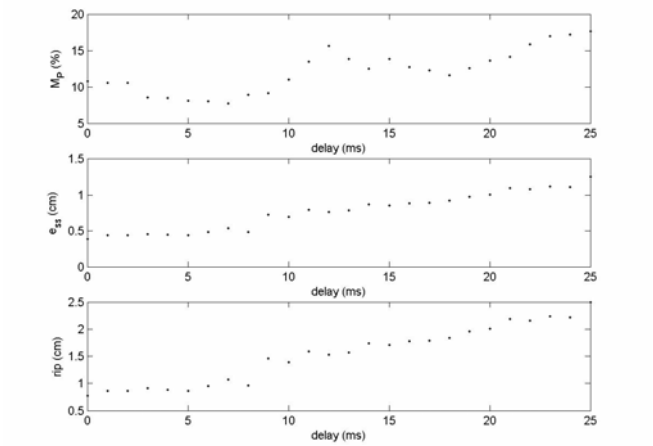

Fig. 3. Maximum percent overshoot *(M_P)*, steady state error (e_{ss}), ripples *(rip)* peak-to-peak amplitude as a function of the delay of the step response, where d = 0, with duty cycle, with DT, $v_f = 0$, h = 25 ms, for a horizontal propulsion.

Preprint submitted to 27th IEEE EMBS Annual International Conference.
Received May 2, 2005.

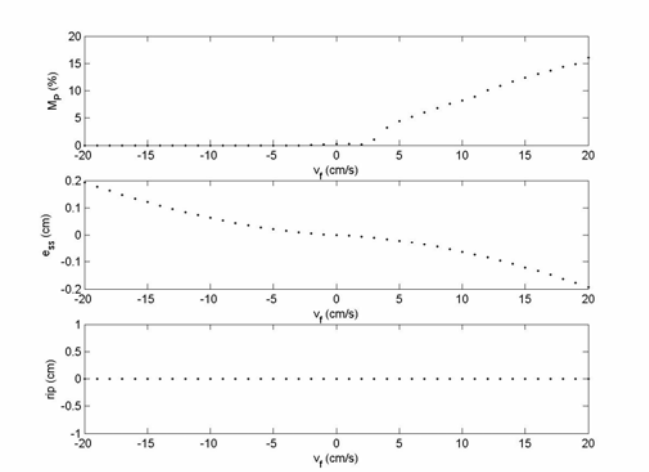

Fig. 4. Maximum percent overshoot (M_P), steady state error (e_{ss}), ripples *(rip)* peak-to-peak amplitude as a function of the fluid speed of the step response, where d = 0 ms, with duty cycle, without DT, h = 25 ms, for a horizontal propulsion.

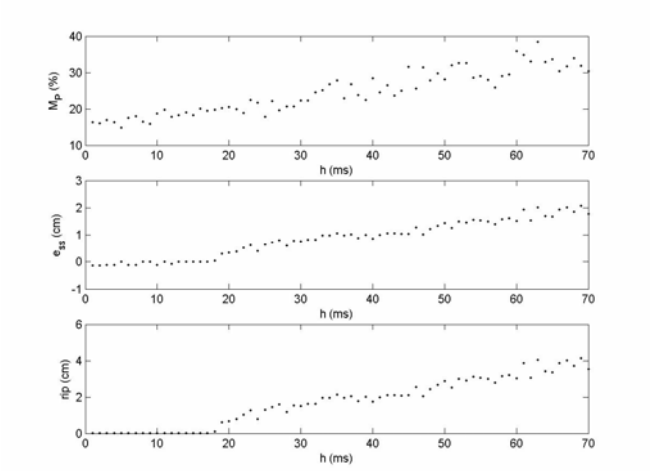

Fig. 5. Maximum percent overshoot *(M_P)*, steady state error (e_{ss}), ripples *(rip)* peak-to-peak amplitude as a function of the sampling time of the step response, where d = 12 ms, with duty cycle, with DT, v_f = 10 cm/s, for a horizontal propulsion.

V. Conclusion

Future developments within the MR-Sub project involve the use of the oximeter to determine the instantaneous fluid speed within the blood vessels at each step in the path. This reading will have to be synchronized along with the roadmap as well as with the pulse prior to intervention. This would definitely render a more robust control. A worthwhile study would be to correlate results between large and small scales models.

Acknowledgment

This work is supported by a strategic grant from the Natural Sciences and Engineering Research Council of Canada (NSERC) and in part by a Canada Research Chair (CRC) in Conception, Fabrication, and Validation of Micro/Nanosystems, the Canadian Foundation for Innovation (CFI), and the Government of Québec. We acknowledge the support of Hôpital Notre-Dame and Centre Hospitalier de l'Université de Montréal (CHUM) that provides the infrastructure to conduct MRI tests.

The authors would like to thank particularly Jean-Baptiste Mathieu, Ouajdi Felfoul, Arnaud Chanu for their suggestions and their readiness in information supply, as well as Pascal Hannoyer for his help with Simulink.

References

[1] J.-B. Mathieu, S. Martel, L. Yahia, G. Soulez, and G. Beaudoin, "Preliminary studies for using magnetic resonance imaging systems as a mean of propulsion for microrobots in blood vessels and evaluation of ferromagnetic artefacts," *Canadian Congress on Electrical and Computer Engineering (CCECE),* Montreal, Canada, pp. p 835-838, 2003.

[2] J.-B. Mathieu, G. Beaudoin, and S. Martel, Method of propulsion of a ferromagnetic core in the cardiovascular system through magnetic gradients generated by an MRI system *IEEE Transactions in BioMedical Engineering*, 2005 (in press).

[3] J.-B. Mathieu, S. Martel, L. Yahia, G. Soulez, and G. Beaudoin, "MRI Systems as a Mean of Propulsion for a Microdevice in Blood Vessels," *IEEE Engineering in Medicine and Biology Society,* Cancun, pp. 3419-3422, Sept. 2003.

[4] J.-B. Mathieu, S. Martel, L. Yahia, G. Soulez, and G. Beaudoin, Preliminary Investigation of the Feasibility of Magnetic Propulsion for Future Microdevices in Blood Vessels *BioMedical Materials and Engineering*, 2005 (in press).

[5] W. Sabra, M. Khouzam, and S. Martel, "Use of 3D Potential Field and an Enhanced Breadth-first Search Algorithms for the Path Planning of Microdevices Propelled in the Cardiovascular System," *27th Conference of the IEEE Engineering in Medicine and Biology Society ,* Shanghai, China, 2005.

[6] A. O'Dwyer, *Handbook of PI and PID controller tuning rules*, New Jersey: World Scientific, 2003.

[7] G. S. Virk, *Digital computer control systems*, New York: McGraw-Hill, 1991.

[8] G. H. Ellis, *Control system design guide a practical guide: [using your computer to understand and diagnose feedback controllers]*, Amsterdam: Elsevier Academic Press, 2004.

[9] K. Ogata, *Modern control engineering*, Upper Saddle River, N.J: Prentice-Hall, 2002.

[10] A. Chanu, S. Martel, and G. Beaudoin, "Real-time Magnetic Resonance Gradient-based Propulsion of a Wireless Microdevice Using Pre-Acquired Roadmap and Dedicated Software Architecture," *27th Conference of the IEEE Engineering in Medicine and Biology Society ,* China, 2005.